Gemini surfactant as multifunctional corrosion and biocorrosion inhibitors for mild steel

PAKIET, M., KOWALCZYK, I., LEIVA GARCIA, R., MOORCROFT, R., NICHOL, Tim <http://orcid.org/0000-0002-0115-957X>, SMITH, Thomas <http://orcid.org/0000-0002-4246-5020>, AKID, R. and BRYCKI, B.

Gemini surfactant as multifunctional corrosion and biocorrosion inhibitors for mild steel

Marta Pakiet [1,2,3], Iwona Kowalczyk[1], Rafael Leiva Garcia[2], Robert Moorcroft[2], Tim Nichol[3], Thomas Smith[3], Robert Akid[2], Bogumił Brycki[1]*

[1] Laboratory of Microbiocides Chemistry, Faculty of Chemistry, Adam Mickiewicz University, Umultowska 89b, 61-614 Poznań, Poland

[2] School of Materials, University of Manchester, Manchester, M13 9PL, UK

[3]Sheffield Hallam University, Howard Street, Sheffield, S1 1WB, UK

*corresponding author
e-mail address: mpakiet@amu.edu.pl

Biocorrosion is an important type of corrosion which leads to economic losses across oli and gas industries, due to increased monitoring, maintenance, and a reduction in platform availability. Anaerobic sulfate reducing bacteria (SRB) are known to accelerate the rate of corrosion tenfold, by secreting specific enzymes. Mitigation strategies include: (i) cleaning procedures; (ii) addition of microbiocides; (iii) antifouling coatings and (iv) cathodic protection. Ideally, a chemical compound engineered to mitigate against biocorrosion would possess both antimicrobial properties, as well as efficient corrosion inhibition. Gemini surfactants have shown efficacy in both of these properties, however there still remains a lack of electrochemical information regarding biocorrosion inhibition.

The inhibition of corrosion and biocorrosion, by cationic gemini surfactants, of carbon steel was investigated. The results showed that the inhibition efficiency of the gemini surfactants was high (consistently > 95 %), even at low concentrations, with the most efficient concentration being above the critical micelle concentration (CMC). Gemini surfactants also showed strong antimicrobial activity, with a minimum inhibitory concentration (0.018 mM). Corrosion inhibition was investigated by electrochemical impedance spectroscopy (EIS) and linear polarisation resistance (LPR), with biocorrosion experiments carried out in an anaerobic environment. Surface morphology was analysed using scanning electron microscopy (SEM).

Keywords

Gemini surfactant, carbon steel, corrosion inhibitor, biocorrosion inhibitor

1. Introduction

Degradation of metals in aqueous environments is often the result of corrosion, which can be exacerbated by biological factors. Any environment containing water with dissolved gases and mineral salts has the potential to generate corrosive activity [1][2]. Metal deterioration, stimulated either directly or indirectly by biological processes is defined as biodeterioration, biocorrosion or microbiologically influenced corrosion (MIC). Microbiologically influenced corrosion is responsible for approximately 10% of all metal corrosion [3], with hundreds of millions of dollars spent mitigating MIC globally each year [4]. The type of microorganisms responsible for MIC varies greatly depending on the oxygen concentration (aerobic or anaerobic conditions). However, microorganisms can co-exist in surface biofilms, meaning that various groups of microorganisms are present, contributing to corrosion with different mechanisms. Groups of microorganisms known to contribute to biological corrosion include: sulfate-reducing bacteria (SRB), sulfur-oxidizing bacteria, and acid producing bacteria (APB), bacteria that produce chemically aggressive organic and inorganic acids [5]. Sulfate-reducing bacteria are obligate anaerobes that, instead of oxygen, can use other terminal electron acceptors, for example sulfate. SRBs excrete hydrogen sulfide ions (HS^-), which are then reduced by free protons to generate corrosive dissolved hydrogen sulfide gas (H_2S), identified by its characteristic, rotten egg smell. In closed systems, such a storage tanks, H_2S can be produced in considerable quantities, posing a serious hazard, especially for the oil industry, both in terms of corrosion and human health during maintenance [6].

The presence of SRB in an anaerobic, aqueous environment, can increase the rate of corrosion fourfold when compared to oxygenated conditions [7]. In aerobic conditions however, an initial population of aerobic bacteria can consume oxygen creating an anaerobic environment in the centre of the biofilm [8,9]. Once locally anaerobic conditions form, SRB can grow and reproduce, using nutrients excreted by the aerobic bacteria. Consequently, SRB initiate MIC, creating incrustations and later pits [1,10].

SRB are considered the most predominant group of microorganisms responsible for MIC. Control of their growth (for example using biocides) once a biofilm is formed, is extremely difficult due to the various natural defences of a biofilm. Extracellular polymeric substances (EPS) create a diffusion barrier[2], and often contain quorum sensing molecules which indicate to other bacteria that they are under attack, and to form protective spores.

Biocorrosion inhibitors are one way to tackle MIC [11,12], however, such compounds, as well as being effective corrosion inhibitors must also possess antimicrobial properties. Gemini

surfactants are amphiphilic compounds, consisting of a hydrophilic head and a hydrophobic tail (**Figure 1a**.), and show both antimicrobial [15,16] and corrosion inhibition properties [13,14].

Synthesized compounds include different lengths of alkyl chain and spacer. Hexamethylene-1,6-bis(*N,N* dimethyl-*N*-dodecyloammonium bromide) (12-6-12) shows the best antifungal activity. 12-6-12 has two quaternary ammonium atoms and long alkyl chain (C_{12}), and given its antifungal activity, was investigated for corrosion inhibition [16]. Surfactants are present in diluted concentrations in single-form molecules, i.e. monomers. When the concentration of these substances in the solution increases, then, at a defined concentration, molecular associations, called micelles, are formed, whereby the solution passes from the solution to the colloidal form. At this concentration, termed the critical micelle concentration (CMC), the physical properties of the solution change rapidly due to the formation of these associations. In solutions with surfactant concentrations above the CMC, micelles are thermodynamically stable and equilibrium with monomers (**Figure 1b.**). The highest corrosion inhibiting efficiency is obtained at concentrations close to the CMC [17,18]. Initially, the surfactant molecules adsorb at the solution / metal interface, reducing the surface tension and forming a protective monolayer. It is this stage that is associated with the prevention of corrosion. At concentrations close to the CMC, the phase boundary is saturated, and micelles or multilayers begin to form in the solution. Further increasing the concentration of inhibitor has limited effects on efficiency [19].

Gemini surfactants are now recognised as multifunctional compounds, because of their many applications: e.g. detergents, solubilisers, biocides, and disperser agents, and now more recently, corrosion inhibitors [14,17–21]. Cationic surfactants are very efficient inhibitors because the positive charge causes strong attachment to metal surfaces [12,14,18,25].

However, investigations into the application of gemini surfactants as biocorrosion inhibitors is limited, and there is a lack of electrochemical information about their ability to mitigate biological corrosion [11,12]. Biocorrosion on carbon steel has been well studied, [9,26] however, this study aims to examine the effects of gemini surfactants on pretreated carbon steel with iron phosphates. The phosphating procedure is used as a pretreatment for additional applications such as coatings, paintings or lubricants, and therefore ubiquitously present.

Therefore, the antimicrobial, and inhibitive properties of the gemini surfactants have been studied using electrochemical impedance spectroscopy (EIS), linear polarisation resistance (LPR), and open circuit potential (OCP). Further characterisation with scanning electron

microscopy (SEM) provides additional evidence for the ability of gemini surfactants to provide protection by corrosion inhibition.

2. Materials and experimental methodology

2.1. Synthesis of cationic surfactant

The surfactant inhibitor was synthesised in accordance with previous work [16]. *N,N*-dimethyl-*N* dodecylamine (9.1 g, 0,045 M) was mixed with 1,6-dibromohexane (5 g, 0.02 M) in acetonitrile (30 mL). The reaction mixture was heated under reflux for 5 h. The solvent was evaporated under reduced pressure and the residue dried over P_4O_{10} and then recrystallized from acetonitrile, with a yield of 84%, m.p. 231-232 °C

The structure of the surfactant (**Figure 2.**) was determined using ^{1}H and ^{13}C NMR [16].

2.2. Mild steel

Pre-phosphated mild steel coupon were used. The composition (in weight %) of the steel is: 0.10 % C, 0.60 % Mn, 0.03 % P, 0.035 % S, 0.2 % Cu, 0.2 % Ni and 0.15 % Cr. Panels were pretreated with Bonderite M-FE 1000. Phosphating is used to modify the surface of ferrous and nonferrous materials. This process is widely used in different types of industry [15,16].

2.3. Characterisation of inhibition properties

Electrochemical analysis was carried out using a conventional three electrode cell with a platinum counter electrode, a saturated calomel electrode (SCE) as a reference electrode and mild steel as the working electrode. The carbon steel was immersed over a period of 24 h in 3.5% NaCl medium with or without inhibitor additions. All tests were repeated in triplicate, with one representative example of every experiment being presented.

2.3.1. Electrochemical measurements

All electrochemical measurements were conducted using a potentiostat (Versastat™ 4.0). Continuous OCP measurements were made over a 24h period. After the 24h OCP measurements, Linear polarization measurements (LPR) and Electrochemical Impedance Spectroscopy (EIS) were recorded. Linear polarization resistance measurements (LPR) were obtained by changing the potential from −20 to +20 mV versus the measured open circuit potential (OCP) with a scan rate of 10 mV min^{-1}. EIS measurements were registered on a frequency range of 10 KHz to 10 mHz with a sine wave perturbation of 10 mV vs OCP. In order to determine cathodic and anodic kinetics, individual separate anodic and cathodic potentiodynamic polarisation measurements were obtained by changing the electrode potential

automatically from OCP to −300 mV (cathodic) vs the OCP and OCP to +300 mV (anodic) vs the OCP, respectively, with a scan rate 0.5 mV s^{-1}.

2.3.2. Surface analysis

The morphology of the carbon steel surface before and after 24 hours immersion was studied by scanning electron microscopy (SEM) using a FEI Quanta 200 operating at 20 kV and different magnifications. Metal samples were rinsed with ethanol and dried at 30 °C prior to immersion and after 24 hours immersion.

2.4. Biocorrosion experimental design

2.4.1. Electrochemical measurements

All electrochemical tests were carried out in a nitrogen filled glove box (< 10 ppm O_2) by constant flow of nitrogen over the 12 days, and carried out at room temperature with continuous immersion of the electrodes. Electrochemical tests were carried out using a platinum counter electrode (CE), a saturated calomel electrode (SCE) as a reference electrode and a working electrode of mild steel (WE). OCP was recorder prior to EIS measurements which were determined at selected interval during the immersion period. The parameters of the EIS scans were the same than those used in section 2.3.1.

In order to better ascertain inhibitor characteristics on the biotic systems, different concentrations were used. **Table 1** shows the four types of cells used in experiment. The blank cell consists of Postgate B medium. The control cell contained Postgate B medium innoculated with *D. salexigens*. Cells one and two consisted of Postgate B medium, the inoculum, and surfactants, with the Critical Micelle Concentration reported in the literature [29], and the Minimal Inhbitory Concentration value determined experimentally respectively. The literature CMC value was also chosen for its known corrosion inhibition efficiency [18]. The final preparation of all the cells was carried out inside the glovebox after 24 hours of purging with nitrogen the closed glovebox.

2.4.2. SRB growing conditions

Desulfovibrio salexigens (DSM 2638, obtained from the Deutsche Sammlung von Mikroorganismen) was used in this study, for its ability to grow in a high saline environment. *D. salexigens* was cultivated in Postgate B medium [30], with the following composition per litre of water, (prepared aerobically): sodium lactate, 3.5 g; yeast extract, 1.0 g; NH_4Cl, 1.0 g; K_2HPO_4, 0.5 g; $MgSO_4$, 2.0 g; $CaSO_4$, 1.0 g; $FeSO_4$, 0.5 g; sodium ascorbate, 0.1 g; sodium thioglycollate, 0.1 g. The medium was pH adjusted to 7.0-7.5 using NaOH, then sterilised by autoclaving at 121°C for 15 min.

2.4.3. Minimal Inhibitory Concentration determination

Increasing concentrations of gemini surfactant were added to 10 ml Postgate B medium in Hungate tubes, with 1 ml inoculum added. When SRBs are cultivated in Postgate B medium, a black iron sulfide precipitate is produced, indicating growth (**Figure 3.**). Minimal inhibitory concentration was determine by standard 2-fold dilution method reported in the literature [31].

3. Results and discussion

3.1. Corrosion inhibition efficiency of the corrosion on mild steel

3.1.1. Open Circuit Potential

Open circuit potential measurements were obtained at room temperature using mild steel samples in 3.5% NaCl with the addition of different concentrations of 12-6-12, as well as a control. **Figure 4** shows the OCP trend with time.

The mild steel potential after 0.5 h was – 604 mV_{SCE} and reached – 625 mV_{SCE} after 24 h of immersion, being stable during the immersion tests. When the inhibitor was added to the solution, the registered potential was more positive for all the concentrations compared to the control.

After 24 hours immersion, the observed potential was similar for all four concentrations of inhibitor, and higher than the control.

The increase in potential is related to the formation of oxide layers on the metal surface. The addition of quaternary ammonium salt further shifts the potential towards more positive values, making the metal surface more resistant to corrosion than the control immersed in the solution, without inhibitor additives.

3.1.2. Potentiodynamic measurements

Figure 5 presents the anodic and cathodic polarisation curves for samples immersed in solutions containing 3.5% NaCl in the presence of the different concentrations of 12-6-12.

Comparing these results with the potentiodynamic curves obtained with the control, it can be observed that both the anodic and the cathodic current densities decrease in the presence of the surfactants, indicating that these compounds suppressed both the anodic and the cathodic reactions through adsorption on the mild steel surface and act as mixed type inhibitor.

3.1.3. Linear Polarisation Resistance

Linear polarization resistance (LPR) is a non-destructive technique, commonly used in corrosion studies to elucidate the corrosion trend of the material in different solutions.

The value of corrosion current density was determined indirectly by measuring the polarization resistance (R_P) and then using the Stern – Geary equation (1) [32]

$$i_{corr} = \frac{\beta_a \beta_c}{2.303(\beta_a + \beta_c)R_P} \quad (1)$$

Where β_a, β_c – are the anodic and cathodic Tafel slopes coefficients of the anode and cathode part of the Tafel chart [V/dec] respectively, and R_P – is the polarisation resistance [Ωcm^2].

Corrosion current density can be translate a into the corrosion inhibition efficiency (IE) using following equation[33–35]:

$$IE\ (\%) = \frac{i_{0\ corr} - i_{corr}}{i_{0\ corr}}\ x\ 100\% \quad (2)$$

Where $i_{0\ corr}$ and i_{corr} are the corrosion current densities with and without the surfactant inhibitor respectively.

Corrosion rate was calculated using the expression given [36,37] (3):

$$CR = \frac{i_{corr}\, Aw\ 10*3.15*10^7}{nFd} \quad (3)$$

Where i_{corr} is the current density [Acm^{-2}], Aw – 56 [g mol^{-1}] for iron, F – Faraday's constant (96 500 $Cmol^{-1}$), n=2, d – density of mild steel (7.85 g cm^{-3}), 3.15 * 10^7 – one year in seconds and 10 is a cm to mm conversion factor.

Polarisation resistance can be determined using the gradient of the potential versus current plot. From the results observed in **Table 2** it can be established that the corrosion inhibitor is effective in reducing corrosion on the carbon steel immersed in the 3.5 % NaCl solution.

Corrosion current density was a maximum for the mild steel sample immersed in 3.5% NaCl without inhibitor at 119.69 [$\mu A/cm^2$]. Increasing the concentrations of corrosion inhibitor caused a significant decrease in current density. The minimum value (0.84 [$\mu A/cm^2$]) was reached in 2mM concentration of 12-6-12. This is because the gemini surfactant was offering protection from corrosion, and the rate of electrochemical reactions was very slow, due to adsorption process. Inhibition efficiency was obtained from the corrosion current density values (Equation 1). From the data in **Table 2**, can be observed that IE increases with increasing concentration of the inhibitor. The chosen concentration was related to CMC value, because this concentration should have the highest inhibition efficiency[17]. 12-6-12 reached the CMC value at 1mM, which was reported previously [38]. Increasing concentration above CMC did not cause a significant change in IE: from 98.7% (1mM) to 99.3%(2mM). In all concentrations investigated, the observed values of IE were above 95 %. Inhibitor is highly efficient even at very low concentration (0.01mM) and reached 95.2%. Corrosion current density is correlated to the corrosion rate (CR) value using (Equation 3).

The corrosion rate of the sample immersed in 3.5% NaCl gave the highest value of 1.39 [mm/year]. The addition of corrosion inhibitors significant decrease the CR and reached a minimum value of 0.010 [mm/year] in 2mM of 12-6-12.

3.1.3. Electrochemical Impedance Spectroscopy

Figure 6 shows Nyquist plots of steel after 24 hours of immersion in a 3.5% NaCl solution at 25 °C with different concentrations of gemini surfactants around the CMC value. It can be observed that the size of the semicircle, clearly larger with the higher concentration of inhibitor. In order to obtain quantitative parameters, the EIS data was fitted to an equivalent circuit as known in **Figure 7**. The proposed equivalent circuit consists of the following elements; RS being the solution resistance (R1), a constant phase element (CPE 1), which corresponds to the capacitive behaviour of the iron phosphate film in parallel with the resistance of the defects on the coating. The second constant phase element (CPE 2) is related to the interface between the metal and the solution in the defects. An additional resistance (R2) in parallel with CPE 2 relates to the resistance of the double layer, which changes with the addition of the inhibitor, which forms a protective film. As the system is not an ideal capacitor, constant phase elements (CPE) are used instead of the capacitors. CPE is transformed into Cdl using Equation 4 [39]:

$$C = \frac{(CPE * R)^{1/\alpha}}{R} \quad (4)$$

n - is the phase shift representing the degree of non-ideality

Inhibition efficiency (IE) was calculated according to the following equation[40–42]

$$IE\ \% = \frac{R_P - R_{OP}}{R_P}\ 100\% \quad (5)$$

where R_{0P} and R_P are the polarisation resistance values, without and with inhibitors for mild steel in 3.5% NaCl, respectively.

The polarisation resistance (Rp) of the system is calculated as the sum of R1 and R2. The results obtained from the fitting are summarised in **Table 3**.

An increase in the value of R2 results from the addition of inhibitor to the solution, which forms a layer between the electrolyte and the metal substrate. In addition, a small increase of the solution resistance on the pores of the iron phosphate is observed due to the presence of the inhibitor. The capacitance values of the phosphate do not change significantly between solutions, while a clear decrease in the capacitance value of the double layer/inhibitor barrier is observed with an increasing concentration of inhibitor, being indicative of a thicker layer

between metal and electrolyte. This effect is clearly noticeable in the region *d* when the CMC value is reached.

Regarding the IE, the values obtained from EIS data are high and show a similar trend to those obtained by LPR measurements.

3.1.4. Adsorption model

Adsorption isotherms provide information showing the interaction between the metal surface and the surfactant molecules, as the corrosion inhibition process appears to be based on displacing water molecules from the surface and replacing them with surfactant molecules on the mild steel surface. Experimental data was fitted to Langmuir adsorption isotherm and found as the most suitable mechanism of corrosion inhibition by the gemini surfactant (**Figure 8.**).
The amount of inhibitor molecules which cover the metal surface can be expressed by the degree of surface coverage (θ). The value of θ for different concentrations of inhibitor in 3.5% NaCl media, have been evaluated using following equation [20,43,44]:

$$\theta = \frac{IE\%}{100} \quad (6)$$

Where the IE% is the inhibition efficiency calculated from LPR. The relationship between θ and IE% appears to be linear [45].
The values of the regression coefficient (R^2) confirmed the validity of this approach, providing a value of 0.9999. This shows that the surfactant formed a single molecule adsorbed layer on the mild steel surface, with no chemical reaction between the adsorbed molecules.

The change in the Gibbs free energy (ΔG_{ads}) was determined using the following equation [46–48]

$$\Delta G_{ads} = -RT\ln(55.5K_{ads}) \quad (7)$$

Where R is the gas constant, T is the temperature and K_{ads} equilibrium adsorption constant is determined by extrapolating the Langmuir isotherm using a linear regression method.
Table 4 summarises the calculated thermodynamic adsorption parameters, based on the data obtained from the LPR.

3.1.5. Surface analysis

The surface morphology of the mild steel samples immersed in 3.5% NaCl solutions for 24 h, containing different concentrations of surfactant was examined by SEM. As shown in **Figure 9,** the mild steel sample before immersion is smooth and without pits (**Figure 9a**). The

distinguishing features are the crystal structure of iron phosphate pre-treatment process. Close examination of the SEM micrographs presented in **Figure 9b** revealed corrosion products and a rougher surface than before immersion. After immersion in medium with 1mM and 2mM of 12-6-12 in 3.5% NaCl, the surface is smooth, and the iron phosphate crystals remain unaffected **(Figure 9c, Figure 9d).** This indicates that the compound reduced the rate of corrosion and greatly reduced the rate of reactions that take place on the mild steel surface. This is attributed to the effective adsorption of the corrosion inhibitior.

4. Biocorrosion

Microbiologically Influenced Corrosion (MIC) is based on the consumption of hydrogen, organic compounds or solid iron as the electron donor, and sulfate as the electron acceptor, being reduced to sulfide. In this respect Von Wolzogen Kuhr and Van der Vlugt suggested the following overall corrosion reaction [49]

$$4Fe + SO_4^{2-} = 3Fe(OH)_2 + FeS + 2OH^- \quad (8)$$

The reaction is defined as the cathodic depolarization theory (CDT). SRB continuously consume atomic hydrogen that accumulates at the cathodic site by hydrogenases. Consequently, this leads to an increase in metal dissolution. The explanation of these results was attributed to the EPS which has the ability to entrap metal ions by binding carboxylic groups of the exopolysaccharides and phosphate groups of the nucleic acids. This binding would affect the electrochemical properties of metal via formation of metal corrosion cells and galvanic coupling on the metal surface.

Understanding biocorrosion requires a knowledge of how the biofilm forms and how metabolic activity induces modifications of the metal surface and how such modifications result in changes to the rates of corrosion [8]. Electrochemical methods offer an insight as to how surfactants can affect the biocorrosion process. The immersion time for electrochemical measurements was correlated with life cycle of SRB. *D. salexigans* enters the log phase of growth at day 4, then enters the stationary phase of growth at day 8 [2].

4.1. Determination of Minimal Inhibitory Concentration

Minimal inhibitory concentration is the lowest concentration of the biocidal agent (antibiotic or chemotherapeutic agent) where antimicrobial activity is observed. Determination of this value was the starting point in this biocorrosion study.

Serial dilutions of 12-6-12 was prepared including range of concentrations. After visual observation based on the control probes (**Figure 3.**), the minimal inhibitory concentration was determined (**Figure 10.**). The value was between the concentrations where growth is and is not observed – equal to 0.018mM. Apart from the SRB, minimal inhibitory concentration was also determined for *A.niger* ATCC 16404, *P.chrysogenum* LOCK 0531, *A.niger* LOCK 0439, *C.albicans* ATCC 10231 in previous studies [16].

4.2. Open Circuit Potential

Open circuit potential (OCP) variations are shown in **Figure 11.** After the first day E_{corr} values start to increase, then (after the 5th day) it begins to stabilise. The shift reaches a stable value at the stationary phase of the bacteria growth cycle [50]. The shift to positive potentials is correlated with the growth of *D. salexigens* [50]. This positive shift in E_{corr} is known as ennoblement. The potential shift suggests that the activity and the growth of the SRB species have enhanced the redox quality of the medium and accelerated the iron dissolution [50]. The SRB attached to the metal surface, forming colonies which form a biofilm. The aggressiveness factors of the biofilm and the active metabolisms of the sessile bacteria alter the electrochemical process; subsequently, producing H_2S and introducing multiple cathodic reactions. The ennoblement has been acknowledged by different investigators as the most notable phenomenon in the development of biocorrosion [50,51]. Ennoblement has been attributed to the microbial colonisation and biofilm formation, which collectively results in organometallic catalysis and acidification of the electrode surface [52]

The reduction in OCP was enhanced and accelerated by the anodic dissolutions. From day 7, bacteria started to show visible signs of growth (evidence as black precipitate), and between day 5 and day 7 E_{corr} stabilises.

4.3. EIS measurements

The Nyquist plots for EIS measurements of carbon steel coupons exposed to different media with SRB and inhibitors are displayed in **Figure 12**. Additionally, **Figures 13** and **14** represent the Bode diagrams for phase and module respectively. As a general observation, it can be observed that the size of the capacitive semicircles is bigger when the inhibitor is present in the solution. After 7 days the solution containing the *D. salexigens* began to show signs of a black precipitate observed in the solution. The transition between the lag and log phases of the bacteria produced changes in the features of the Nyquist plots. The size of the Nyquist semi-circles decreases as a consequence of the corrosion process favoured by the bacteria and becomes more capacitive due to the formation of the biofilm. In the case of the medium without

bacteria, the size of the Nyquist plots decrease with the immersion time after the second day due to the corrosion process, however this drop is not as noticeable as in the case solution with just the medium with bacteria. On the other hand, when the inhibitor is added a similar effect is observed for both concentrations, first the bacterial activity stops and second the corrosion process is minimised by an order of magnitude.

Figure 13 shows that one time constant at the intermediate frequency is operative for the first 24 h, indicating activation and control process [53]. This behavior is attributed to the formation of an unstable layer based on a mixture of inorganic/organic compounds which are present in the medium. The first three graphs show similar behavior (**Figure 13a, 13b, 13c**). In the case of the medium with bacteria (**Figure 13d**), differences can also be observed after 7 days, when the mature biofilm formed. The impedance shifts to higher frequency, which is related to the growth of bacteria [54,55]. The time constant at the high frequency might be due to the formation of composite films containing a combination of corrosion product and biofilm [56].

The experimental data was fitted to the equivalent circuit shown in **Figure 7,** using ZView2© [57]. The proposed equivalent circuit consists of a solution resistance (R1), a constant phase element (CPE1), relating to the capacitive behavior of the film on the metal surface in parallel with a resistance (R2), constant phase element (CPE2) and resistance (R3) of the metal surface. The charge transfer resistance obtained from fitting the EIS data to the equivalent circuit are presented in **Table 5**.
As explained previously, CPE elements where used to take into account the non-ideal behaviour of the capacitors, with equation 4 being used to obtain the capacitance values.

From the results presented in **Table 5,** differences in the corrosion processes taking place can be observed between the medium with and without bacteria. In the case of the abiotic medium, the resistance of the phosphate layer on the steel surface, decreases with time, while the charge transfer resistance increases to 26 KΩ cm^2 after 8 days, decreasing after 12 days to 20 KΩ cm^2. This increase in the polarization resistance is a consequence of the presence of other compounds in the Postgate B medium, which were not present in the sodium chloride solution, and causing an enhance the protection of the metal by interacting with the substrate surface (**Figure 12**). The capacitance values of the outer phosphate coating (C1) remain constant during the entire duration of the experiment, as well as the capacitance values of the double layer (C2). In contrast with these results, when the SRB are added to the solution, a decrease in the film and charge transfer resistance is observed, which is due to the bacterial activity favouring the

corrosion of the metal. Together with the decrease in the corrosion resistance, a clear increase in the capacitance values is shown. This rise in the capacitance values can be associated with two factors: the increase of the interfacial area after the bacteria become metabolically active, resulting from biofilm formation and the secretion of extracellular polymeric substances, or the charging effects, due to the metabolic activity of the bacteria leading to absorption and desorption of compounds on the metallic surface, such as iron sulfide films. Protective iron sulfide films can be found in when hydrogen sulfide is present (as in sour environments) [2,10]. There are always thin films adhered to the surface, however, with the bacterial suspension, the sulfide films are not stable. They are disrupted by the metabolism of the bacteria, for example, excretion of corrosive substances, such as acetic acid. Therefore, with the proliferation of the SRB (and metabolic products), the protective iron sulfide film decomposes to other polysulfide products [58]. The integrity of the protective film then degrades becoming loose and porous. Subsequently, the steel surface was exposed to the corrosive medium, increasing the corrosion rate significantly. During the last stages, when the SRB metabolic activity declined, it would lead to a reduction of the iron to sulfide ratio reducing the hydrogen sulfide film can occur[59].

When the inhibitor was added, it can be noted that even at the critical inhibitory concentration, it is an efficient biocide and corrosion inhibitor. After 12 days, for both concentrations, the corrosion resistance is much greater than without an inhibitor, and no significant increase of the capacitive behavior (which was observed when the SRB were active) was observed. The polarization resistance (R1+R2) for both concentrations after 12 days are similar, indicating that the compound can act as both a corrosion inhibitor and biocide, even at low concentrations.

5. Conclusion

From the results obtained the following conclusions can be drawn:

- The synthesised cationic surfactant 12-6-12 has antibacterial activity against *D. salexigens*.
- The gemini surfactant acts as corrosion inhibitor against mild steel in 3.5% NaCl. Inhibition efficiency (IE) increasing with increasing concentration of the inhibitor. For all concentrations achieved IE values were above 95%. LPR and EIS data were in agreement. In the present study, Langmuir adsorption isotherm was found to be the most suitable model for the system studied.
- 12-6-12 acts as a biocorrosion inhibitor. In the electrochemical cells studied, the only cell to cultivate *D. salexigens* was with media and an inoculum. Neither cell containing 12-6-12 allowed cultivation.

- 12-6-12 is a very efficient surfactant, inhibiting both corrosion and biocorrosion, even in very low concentrations.

Acknowledgements

This work was supported by National Centre for Research and Development (Poland; TANGO1/266340/NCBR/2015).

The authors would also like to thank the School of Materials, University of Manchester and Sheffield Hallam University for providing research facilities.

References

[1] D. Enning, J. Garrelfs, Corrosion of Iron by Sulfate-Reducing Bacteria: New Views of an Old Problem, Appl. Environ. Microbiol. 80 (2014) 1226–1236. doi:10.1128/AEM.02848-13.

[2] T. Liengen, Understanding biocorrosion: fundamentals and applications, Elsevier, Boston, MA, 2014.

[3] I.B. Beech, C.C. Gaylarde, Recent advances in the study of biocorrosion: an overview, Rev. Microbiol. 30 (1999) 117–190.

[4] T.L. Skovhus, R.B. Eckert, E. Rodrigues, Management and control of microbiologically influenced corrosion (MIC) in the oil and gas industry—Overview and a North Sea case study, J. Biotechnol. 256 (2017) 31–45. doi:10.1016/j.jbiotec.2017.07.003.

[5] H.A. Videla, Prevention and control of biocorrosion, Int. Biodeterior. Biodegrad. 49 (2002) 259–270.

[6] J. McKenzie, W.A. Hamilton, The assay of in-situ activities of sulphate-reducing bacteria in a laboratory marine corrosion model, Int. Biodeterior. Biodegrad. 29 (1992) 285–297. doi:10.1016/0964-8305(92)90049-T.

[7] A.L. Tarasov, I.A. Borzenkov, Sulfate-reducing bacteria of the genus *Desulfovibrio* from south vietnam seacoast, Microbiology. 84 (2015) 553–560. doi:10.1134/S0026261715040165.

[8] I.B. Beech, J. Sunner, Biocorrosion: towards understanding interactions between biofilms and metals, Curr. Opin. Biotechnol. 15 (2004) 181–186. doi:10.1016/j.copbio.2004.05.001.

[9] E. Malard, D. Kervadec, O. Gil, Y. Lefevre, S. Malard, Interactions between steels and sulphide-producing bacteria—Corrosion of carbon steels and low-alloy steels in natural seawater, Electrochimica Acta. 54 (2008) 8–13. doi:10.1016/j.electacta.2008.05.075.

[10] T. Gu, New Understandings of Biocorrosion Mechanisms and their Classifications, J. Microb. Biochem. Technol. 04 (2012). doi:10.4172/1948-5948.1000e107.

[11] A. Labena, M.A. Hegazy, H. Horn, E. Müller, The biocidal effect of a novel synthesized gemini surfactant on environmental sulfidogenic bacteria: Planktonic cells and biofilms, Mater. Sci. Eng. C. 47 (2015) 367–375. doi:10.1016/j.msec.2014.10.079.

[12] A. Labena, M.A. Hegazy, H. Horn, E. Müller, Cationic Gemini Surfactant as a Corrosion Inhibitor and a Biocide for High Salinity Sulfidogenic Bacteria Originating from an Oil-Field Water Tank, J. Surfactants Deterg. 17 (2014) 419–431. doi:10.1007/s11743-013-1551-4.

[13] F.M. Menger, C.A. Littau, Gemini-surfactants: synthesis and properties, J. Am. Chem. Soc. 113 (1991) 1451–1452.

[14] B.E. Brycki, I.H. Kowalczyk, A. Szulc, O. Kaczerewska, M. Pakiet, Multifunctional Gemini Surfactants: Structure, Synthesis, Properties and Applications, in: R. Najjar (Ed.), Appl. Charact. Surfactants, InTech, 2017. doi:10.5772/intechopen.68755.

[15] K. Taleb, M. Mohamed-Benkada, N. Benhamed, S. Saidi-Besbes, Y. Grohens, A. Derdour, Benzene ring containing cationic gemini surfactants: Synthesis, surface properties and antibacterial activity, J. Mol. Liq. 241 (2017) 81–90. doi:10.1016/j.molliq.2017.06.008.

[16] B. Brycki, I. Kowalczyk, A. Kozirog, Synthesis, Molecular Structure, Spectral Properties and Antifungal Activity of Polymethylene-α,ω-bis(N,N- dimethyl-N-dodecyloammonium Bromides), Molecules. 16 (2011) 319–335. doi:10.3390/molecules16010319.

[17] M. Pakiet, I.H. Kowalczyk, R. Leiva Garcia, R. Akid, B.E. Brycki, Influence of different counterions on gemini surfactants with polyamine platform as corrosion inhibitors for stainless steel AISI 304 in 3 M HCl, J. Mol. Liq. 268 (2018) 824–831. doi:10.1016/j.molliq.2018.07.120.
[18] O. Kaczerewska, R. Leiva-Garcia, R. Akid, B. Brycki, I. Kowalczyk, T. Pospieszny, Effectiveness of O -bridged cationic gemini surfactants as corrosion inhibitors for stainless steel in 3 M HCl: Experimental and theoretical studies, J. Mol. Liq. 249 (2018) 1113–1124. doi:10.1016/j.molliq.2017.11.142.
[19] F.A. Ansari, M.A. Quraishi, Inhibitive Performance of Gemini Surfactants as Corrosion Inhibitors for Mild Steel in Formic Acid, 28 (2010) 321–335. doi:DOI: 10.4152/pea.201005321.
[20] F. Kellou-Kerkouche, A. Benchettara, S.-E. Amara, Anionic Surfactant as a Corrosion Inhibitor for Synthesized Ferrous Alloy in Acidic Solution, J. Mater. 2013 (2013) 1–11. doi:10.1155/2013/903712.
[21] B.E. Brycki, I.H. Kowalczyk, A. Szulc, O. Kaczerewska, M. Pakiet, Multifunctional Gemini Surfactants: Structure, Synthesis, Properties and Applications, in: R. Najjar (Ed.), Appl. Charact. Surfactants, InTech, 2017. doi:10.5772/intechopen.68755.
[22] A. Tehrani-Bagha, K. Holmberg, Solubilization of Hydrophobic Dyes in Surfactant Solutions, Materials. 6 (2013) 580–608. doi:10.3390/ma6020580.
[23] H. Nakahara, Y. Kojima, Y. Moroi, O. Shibata, Solubilization of *n* -Alkylbenzenes into Gemini Surfactant Micelles in Aqueous Medium, Langmuir. 30 (2014) 5771–5779. doi:10.1021/la501519a.
[24] A. Koziróg, D. Kręgiel, B. Brycki, Action of Monomeric/Gemini Surfactants on Free Cells and Biofilm of Asaia lannensis, Molecules. 22 (2017) 2036. doi:10.3390/molecules22112036.
[25] B.E. Brycki, I.H. Kowalczyk, A. Szulc, O. Kaczerewska, M. Pakiet, Organic Corrosion Inhibitors, in: M. Aliofkhazraei (Ed.), Corros. Inhib. Princ. Recent Appl., InTech, 2018. doi:10.5772/intechopen.72943.
[26] J. Xu, C. Sun, M. Yan, F. Wang, Effects Of Sulfate-Reducing Bacteria on Corrosion of Carbon Steel Q235 in the Crevice by EIS, Int J Electrochem Sci. 7 (2012) 16.
[27] G. Górecki, Iron Phosphate Coatings—Composition and Corrosion Resistance, CORROSION. 48 (1992) 613–616. doi:10.5006/1.3315980.
[28] R.S. Peres, E. Cassel, C.A. Ferreira, D.S. Azambuja, Grain Refiner Effect of Black Wattle Tannin in Iron and Zinc Phosphate Coatings, Ind. Eng. Chem. Res. 53 (2014) 2706–2712. doi:10.1021/ie403820m.
[29] M.T. Garcia, O. Kaczerewska, I. Ribosa, B. Brycki, P. Materna, M. Drgas, Hydrophilicity and flexibility of the spacer as critical parameters on the aggregation behavior of long alkyl chain cationic gemini surfactants in aqueous solution, J. Mol. Liq. 230 (2017) 453–460. doi:10.1016/j.molliq.2017.01.053.
[30] D.K. Jain, Evaluation of the semisolid Postgate's B medium for enumerating sulfate-reducing bacteria, J. Microbiol. Methods. 22 (1995) 27–38. doi:10.1016/0167-7012(94)00061-B.
[31] Determination of minimum inhibitory concentrations (MICs) of antibacterial agents by broth dilution, Clin. Microbiol. Infect. 9 (2003) ix–xv. doi:10.1046/j.1469-0691.2003.00790.x.
[32] E. Machnikova, K.H. Whitmire, N. Hackerman, Corrosion inhibition of carbon steel in hydrochloric acid by furan derivatives, Electrochimica Acta. 53 (2008) 6024–6032. doi:10.1016/j.electacta.2008.03.021.
[33] P.O. Ameh, N.O. Eddy, Theoretical and experimental studies on the corrosion inhibition potentials of 3-nitrobenzoic acid for mild steel in 0.1 M H2SO4, Cogent Chem. 2 (2016). doi:10.1080/23312009.2016.1253904.
[34] S.M. Shaban, A. Saied, S.M. Tawfik, A. Abd-Elaal, I. Aiad, Corrosion inhibition and Biocidal effect of some cationic surfactants based on Schiff base, J. Ind. Eng. Chem. 19 (2013) 2004–2009. doi:10.1016/j.jiec.2013.03.013.
[35] M.O. Agafonkina, N.P. Andreeva, Y.I. Kuznetsov, S.F. Timashev, Substituted benzotriazoles as inhibitors of copper corrosion in borate buffer solutions, Russ. J. Phys. Chem. A. 91 (2017) 1414–1421. doi:10.1134/S0036024417080027.
[36] F.A. Ansari, M.A. Quraishi, Inhibitive performance of gemini surfactants as corrosion inhibitors for mild steel in formic acid, Port. Electrochimica Acta. 28 (2010) 321–335.

[37] D. Zhang, L. Gao, G. Zhou, Inhibition of copper corrosion in aerated hydrochloric acid solution by heterocyclic compounds containing a mercapto group, Corros. Sci. 46 (2004) 3031–3040. doi:10.1016/j.corsci.2004.04.012.
[38] B. Brycki, M. Drgas, M. Bielawska, A. Zdziennicka, B. Jańczuk, Synthesis, spectroscopic studies, aggregation and surface behavior of hexamethylene-1,6-bis(N,N-dimethyl-N-dodecylammonium bromide), J. Mol. Liq. 221 (2016) 1086–1096. doi:10.1016/j.molliq.2016.06.075.
[39] R. Leiva-García, J.C.S. Fernandes, M.J. Muñoz-Portero, J. García-Antón, Study of the sensitisation process of a duplex stainless steel (UNS 1.4462) by means of confocal microscopy and localised electrochemical techniques, Corros. Sci. 94 (2015) 327–341. doi:10.1016/j.corsci.2015.02.016.
[40] Y.-J. Tan, S. Bailey, B. Kinsella, An investigation of the formation and destruction of corrosion inhibitor films using electrochemical impedance spectroscopy (EIS), Corros. Sci. 38 (1996) 1545–1561.
[41] M.P. Desimone, G. Grundmeier, G. Gordillo, S.N. Simison, Amphiphilic amido-amine as an effective corrosion inhibitor for mild steel exposed to CO2 saturated solution: Polarization, EIS and PM-IRRAS studies, Electrochimica Acta. 56 (2011) 2990–2998. doi:10.1016/j.electacta.2011.01.009.
[42] A. Jmiai, B. El Ibrahimi, A. Tara, R. Oukhrib, S. El Issami, O. Jbara, L. Bazzi, M. Hilali, Chitosan as an eco-friendly inhibitor for copper corrosion in acidic medium: protocol and characterization, Cellulose. 24 (2017) 3843–3867. doi:10.1007/s10570-017-1381-z.
[43] S. Stolnik, B. Daudali, A. Arien, J. Whetstone, C.R. Heald, M.C. Garnett, S.S. Davis, L. Illum, The effect of surface coverage and conformation of poly (ethylene oxide)(PEO) chains of poloxamer 407 on the biological fate of model colloidal drug carriers, Biochim. Biophys. Acta BBA-Biomembr. 1514 (2001) 261–279.
[44] M.A. Hegazy, M. Abdallah, H. Ahmed, Novel cationic gemini surfactants as corrosion inhibitors for carbon steel pipelines, Corros. Sci. 52 (2010) 2897–2904. doi:10.1016/j.corsci.2010.04.034.
[45] Chem. Dep., Faculty of Applied Sciences, Umm Al-Qura University, Makkah, Saudi Arabia., M. Abdallah, Corrosion Inhibition of Stainless Steel Type 316 L in 1.0 M HCl Solution Using 1,3-Thiazolidin-5-one Derivatives, Int. J. Electrochem. Sci. (2017) 4543–4562. doi:10.20964/2017.05.35.
[46] S. Manimegalai, P. Manjula, Thermodynamic and Adsorption studies for corrosion Inhibition of Mild steel in Aqueous Media by *Sargasam swartzii* (Brown algae), J. Mater. Environ. Sci. 6 (2015) 1629–1637.
[47] M. Abdallah, H.M. Eltass, M.A. Hegazy, H. Ahmed, Adsorption and inhibition effect of novel cationic surfactant for pipelines carbon steel in acidic solution, Prot. Met. Phys. Chem. Surf. 52 (2016) 721–730. doi:10.1134/S207020511604002X.
[48] I. Danaee, O. Ghasemi, G.R. Rashed, M. Rashvand Avei, M.H. Maddahy, Effect of hydroxyl group position on adsorption behavior and corrosion inhibition of hydroxybenzaldehyde Schiff bases: Electrochemical and quantum calculations, J. Mol. Struct. 1035 (2013) 247–259. doi:10.1016/j.molstruc.2012.11.013.
[49] C.A. Loto, Microbiological corrosion: mechanism, control and impact—a review, Int. J. Adv. Manuf. Technol. 92 (2017) 4241–4252. doi:10.1007/s00170-017-0494-8.
[50] Q. Zhang, P. Wang, D. Zhang, Stainless Steel Electrochemical Corrosion Behaviors Induced by Sulphate-Reducing Bacteria in Different Aerated Conditions, Int J Electrochem Sci. 7 (2012) 12.
[51] D. Enning, H. Venzlaff, J. Garrelfs, H.T. Dinh, V. Meyer, K. Mayrhofer, A.W. Hassel, M. Stratmann, F. Widdel, Marine sulfate-reducing bacteria cause serious corrosion of iron under electroconductive biogenic mineral crust: Microbial iron corrosion under electroconductive crust, Environ. Microbiol. 14 (2012) 1772–1787. doi:10.1111/j.1462-2920.2012.02778.x.
[52] F.M. AlAbbas, R. Bhola, J.R. Spear, D.L. Olson, B. Mishra, Electrochemical Characterization of Microbiologically Influenced Corrosion on Linepipe Steel Exposed to Facultative Anaerobic Desulfovibrio sp., Int J Electrochem Sci. 8 (2013) 13.
[53] F.M. AlAbbas, C. Williamson, S.M. Bhola, J.R. Spear, D.L. Olson, B. Mishra, A.E. Kakpovbia, Microbial Corrosion in Linepipe Steel Under the Influence of a Sulfate-Reducing Consortium Isolated from an Oil Field, J. Mater. Eng. Perform. 22 (2013) 3517–3529. doi:10.1007/s11665-013-0627-7.

[54] C. Clausen, M. Dimaki, C. Bertelsen, G. Skands, R. Rodriguez-Trujillo, J. Thomsen, W. Svendsen, Bacteria Detection and Differentiation Using Impedance Flow Cytometry, Sensors. 18 (2018) 3496. doi:10.3390/s18103496.
[55] C. Slouka, G. Brunauer, J. Kopp, M. Strahammer, J. Fricke, J. Fleig, C. Herwig, Low-Frequency Electrochemical Impedance Spectroscopy as a Monitoring Tool for Yeast Growth in Industrial Brewing Processes, Chemosensors. 5 (2017) 24. doi:10.3390/chemosensors5030024.
[56] Y. Qing, Y. Bai, J. Xu, T. Wu, M. Yan, C. Sun, Effect of Alternating Current and Sulfate-Reducing Bacteria on Corrosion of X80 Pipeline Steel in Soil-Extract Solution, Materials. 12 (2019) 144. doi:10.3390/ma12010144.
[57] J. Xu, K. Wang, C. Sun, F. Wang, X. Li, J. Yang, C. Yu, The effects of sulfate reducing bacteria on corrosion of carbon steel Q235 under simulated disbonded coating by using electrochemical impedance spectroscopy, Corros. Sci. 53 (2011) 1554–1562. doi:10.1016/j.corsci.2011.01.037.
[58] M. Zeeshan, Mechanisms of Microbiologically Influenced Corrosion: A Review, (2012) 8.
[59] X. Sheng, Y.-P. Ting, S.O. Pehkonen, The influence of sulphate-reducing bacteria biofilm on the corrosion of stainless steel AISI 316, Corros. Sci. 49 (2007) 2159–2176. doi:10.1016/j.corsci.2006.10.040.

Caption of figures

Figure 1. Schematic representation of (a) gemini surfactant and (b) micelle created from gemini surfactants in aqueous solution.

Figure 2. Structure of hexamethylene-1,6-bis(*N,N*-dimethyl-*N*-dodecyldodecylammonium bromide) (12-6-12).

Figure 3. Hungate's tube filled with Postgate B medium (**a**) and cultivated SRB (**b**).

Figure 4. Open circuit potential – time curves for stainless steel electrode immersed in 3.5% NaCl at room temperature in the absence and presence of different concentration of the gemini surfactant.

Figure 5. Anodic (**A**) and cathodic (**B**) curves for mild steel in 3.5% NaCl with and without different concentrations of 12-6-12 at room temperature.

Figure 6. Nyquist plots of different concentrations of 12-6-12 in 3.5 % NaCl at room temperature after 24 h immersion.

Figure 7. Equivalent circuit diagram for modelling the EIS data.

Figure 8. Langmuir adsorption plot for mild steel in 3.5% NaCl solution containing various concentration of 12-6-12 after 24 h immersion at room temperature.

Figure 9. SEM micrographs of mild steel surface (a) before immersion, (b) after 24 h immersion in 3.5% NaCl (c) after 24h immersion in 3.5% NaCl with 1mM 12-6-12 (d) after 24h immersion in 3.5% NaCl with 2mM 12-6-12.

Figure 10. Representative tubes contained Postgate's B medium, SRB inoculum and increasing concentration of 12 -6-12 (from left to right).

Figure 11. Open Circuit Potential (OCP) variations as a function of time under anaerobic conditions at room temperature.

Figure 12. Nyquist plot of (a) cell 1 (b) cell 2 (c) medium and (d) medium with bacteria dependent on time under inert atmosphere.

Figure 13. Phase angle plots as a function of time for: (a) cell 1 (b) cell 2 (c) medium and (d) medium with bacteria dependent on time.

Figure 14. Modulus plot of (a) cell 1 (b) cell 2 (c) medium and (d) medium with bacteria dependent on time.

Caption of Tables

Table 1. Composition of cells designed for experiment in glove box under anaerobic conditions.

Table 2. Linear Polarisation measurements data after 24 h immersion with and without inhibitors in 3.5% NaCl medium at room temperature.

Table 3. EIS parameters for corrosion inhibitor of carbon steel in 3.5% NaCl in absence and presence of different concentrations of the surfactants (after 24 h) at room temperature.

Table 4. Data obtained from Langmuir isotherm model for 12-6-12 in 3.5% NaCl after 24 h immersion at room temperature.

Table 5. EIS parameters for biocorrosion in Postgate B medium in absence and presence of different concentrations of the surfactants at room temperature under anaerobic conditions.

Table 2. Composition of cells designed for experiment in glove box under anaerobic conditions.

	Postgate's B medium	*Desulfovibrio salexigans*	Concentration of surfactant [mM]
Blank cell	x		
Control cell	x	x	
Surfactant cell – Cell1	x	x	1 – CMC point
Surfactant cell – Cell2	x	x	0.018 – MIC point

Table 2. Linear Polarisation measurements data after 24 h immersion with and without inhibitors in 3.5% NaCl medium at room temperature.

-	Concentration of surfactant [mM]	i_{corr} [µA/cm^2]	Ba [mV/dec]	Bc [mV/dec]	CR [mm/year]	Inhibition efficiency [%]
3.5% NaCl	**0**	**119.69±1.21**	**109±1**	**296±3**	**1.39±0.12**	**-**
12-6-12	**0.01**	**5.79±0.03**	**42±3**	**211±3**	**0.068±0.002**	**95.2±0.2**
	0.1	**1.78±0.23**	**33±2**	**180±3**	**0.021±0.003**	**98.5±0.2**
	1 – CMC point	**1.61±0.34**	**44±3**	**80±3**	**0.019±0.001**	**98.7±0.2**
	2	**0.84±0.01**	**55±2**	**87±3**	**0.010±0.06**	**99.3±0.3**

Table 3. EIS parameters for corrosion inhibitor of carbon steel in 3.5% NaCl in absence and presence of different concentrations of the surfactants (after 24 h) at room temperature.

	Concentration of surfactant [mM]	`Rs [Ω cm^2]	C_1 [µF/cm^2]	α_1	R_1 [Ω cm^2]	C_2 [µF/cm^2]	α_2	R_2 [Ω cm^2]	X^2	Inhibition efficiency[%]	Rp [Ωcm^2]
3.5% NaCl	0	6 ±1	22 ±1	0.69	18 ±2	2388 ±30	0.53	272 ±21	1x10^{-3}	--	289
12-6-12	0.01	22 ±3	32 ±4	0.69	84 ±9	2002 ±40	0.55	2294 ±33	6x10^{-3}	87	2318
	0.1	21 ±4	21 ±1	0.72	84 ±7	285 ±38	0.64	3236 ±41	2x10^{-3}	**91**	3320
	1	23 ±3	25 ±5	0.69	98 ±6	104 ±13	0.61	6270 ±56	7x10^{-3}	95	6368
	2	21 ±3	26 ±3	0.82	427 ±18	20 ±3	0.59	7840 ±45	3x10^{-3}	96	8267

Table 4. Data obtained from Langmuir isotherm model for 12-6-12 in 3.5% NaCl after 24 h immersion at room temperature.

Concentration of surfactant [mM]	Θ	K_{ads} *10^3[dm^3/mol]	ΔG_{ads} [kJ/mol]	R^2	slope
0.01	0.95	0.565±0.087	-25.65±1.21	0.999	1.0072
0.1	0.98				
1	0.98				
2	0.99				

Table 5. EIS parameters for biocorrosion in Postgate B medium in absence and presence of different concentrations of the surfactants at room temperature under anaerobic conditions.

	Days	`Rs [Ω cm^2]	C_1 [µF/cm^2]	α_1	R_1 [Ω cm^2]	C_2 [µF/cm^2]	α_2	R_2 [Ω cm^2]	X^2

Medium	Day 0	6±1	35±2	0.72	2221±18	368±5	0.98	10479±125	$3x10^{-3}$
	Day 8	9±1	16±3	0.77	689±8	177±4	0.87	26019±149	$2x10^{-3}$
	Day 12	8±1	12±3	0.89	21±2	223±23	0.77	20397±150	$3x10^{-3}$
Medium + Bacteria	Day 0	13±1	16.3±5	0.88	1061±19	19±1	0.66	10785±102	$4x10^{-3}$
	Day 8	5±1	3769±196	0.84	498±16	1707±17	0.84	7128±109	$3x10^{-3}$
	Day 12	5±1	15500±208	0.93	567±13	4777±89	0.83	9345±145	$8x10^{-3}$
Cell 1	Day 0	12±2	27±1	0.85	629±2	3±1	0.517	11188±385	$9x10^{-3}$
	Day 8	12±2	15±1	0.86	4634±4	400±23	0.68	45085±249	$8x10^{-3}$
	Day 12	27±5	12±1	0.84	5231±7	436±38	0.54	31676±487	$3x10^{-3}$
Cell 2	Day 0	12±1	23±2	0.9	345±26	87±13	0.77	6418±221	0.03
	Day 8	15±4	60±4	0.852	314±28	196±47	0.63	48577±341	$6x10^{-4}$
	Day 12	16±4	50±6	0.86	3876±111	350±39	0.51	36936±411	$5x10^{-3}$

Figure 1

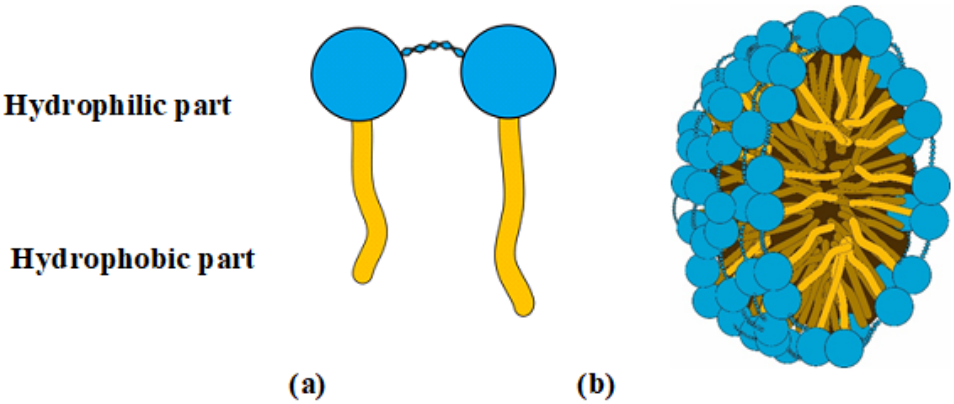

Figure 2

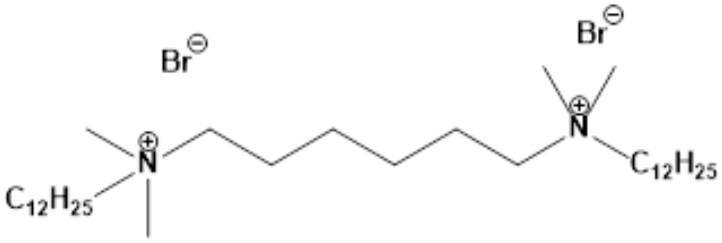

Figure 3

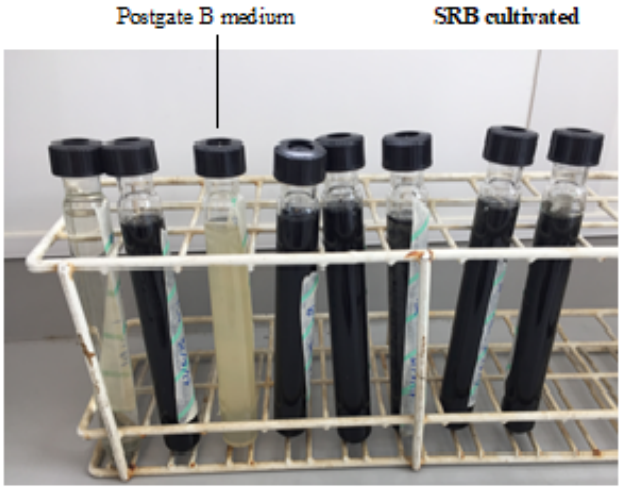

Figure 4

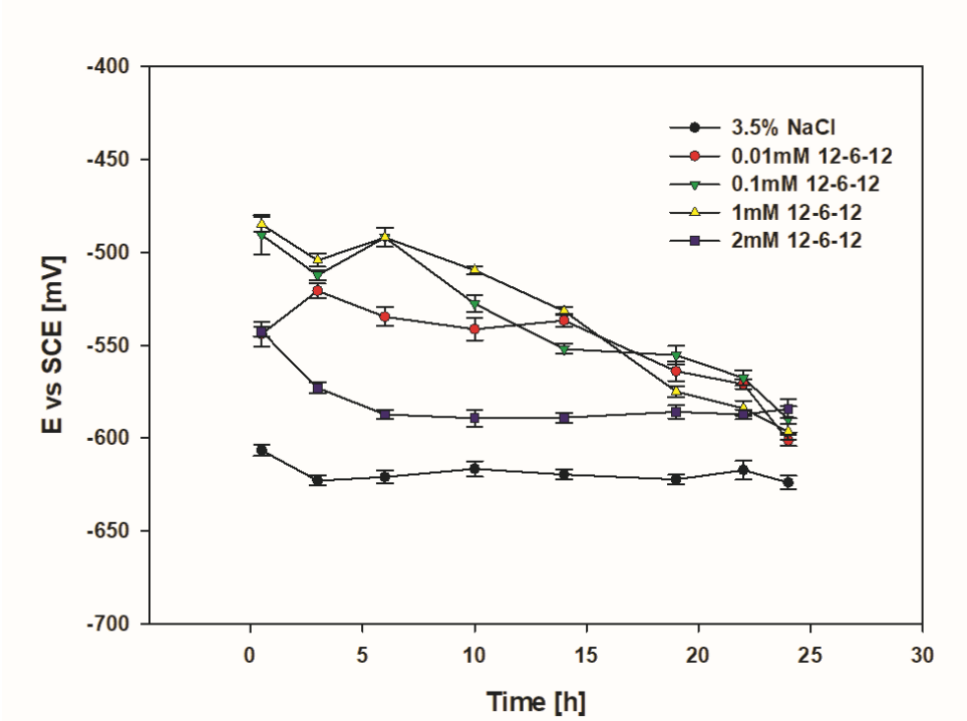

Figure 5

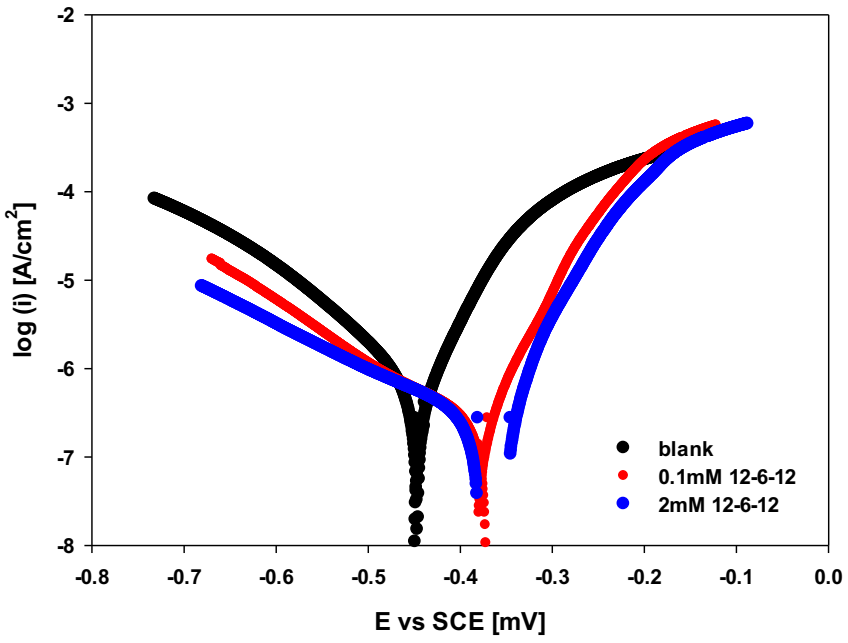

Figure 6

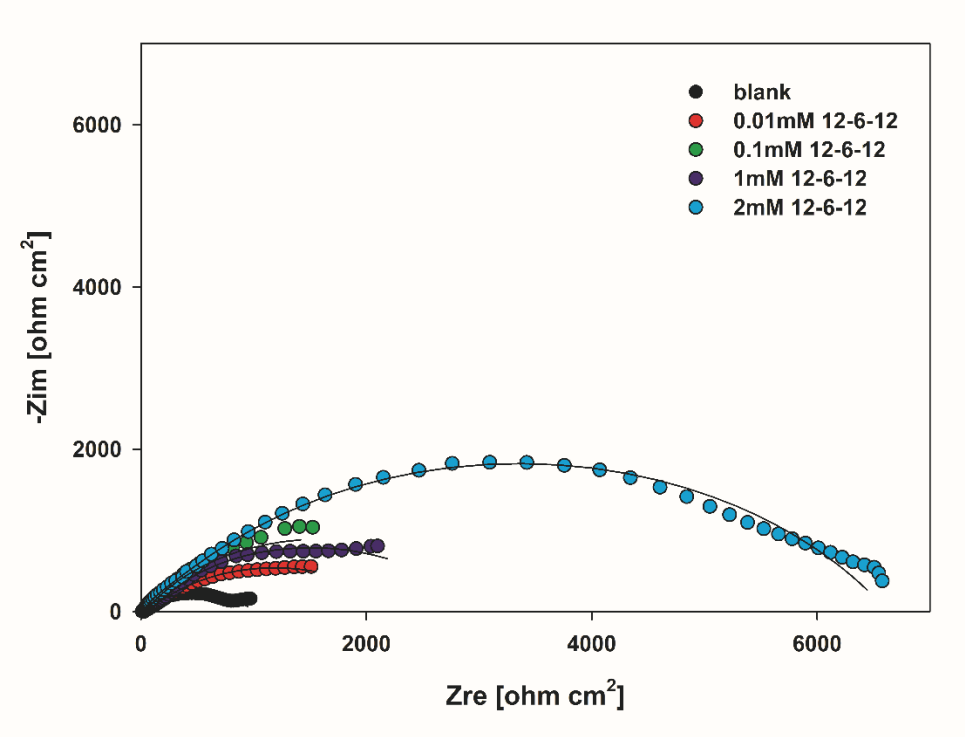

Figure 7

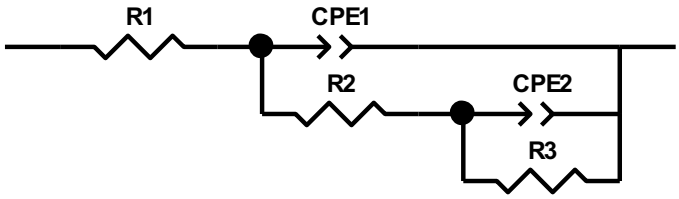

Figure 8

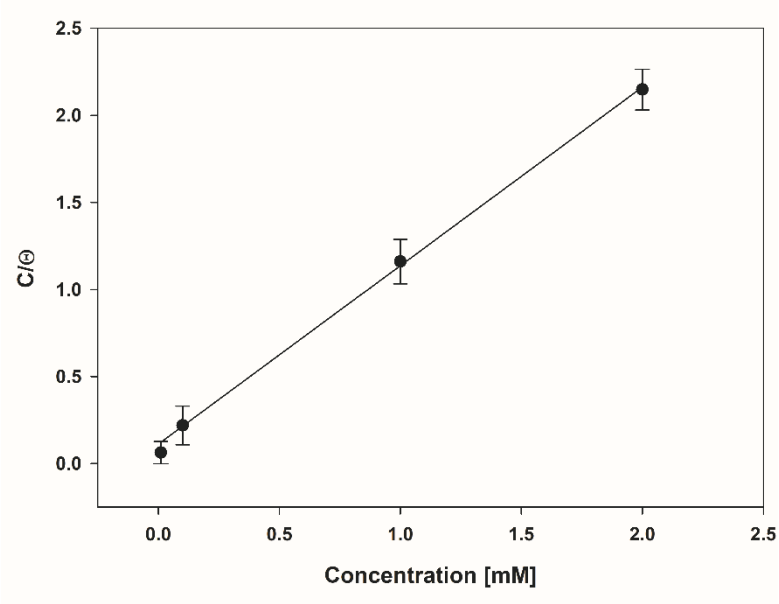

Figure 9

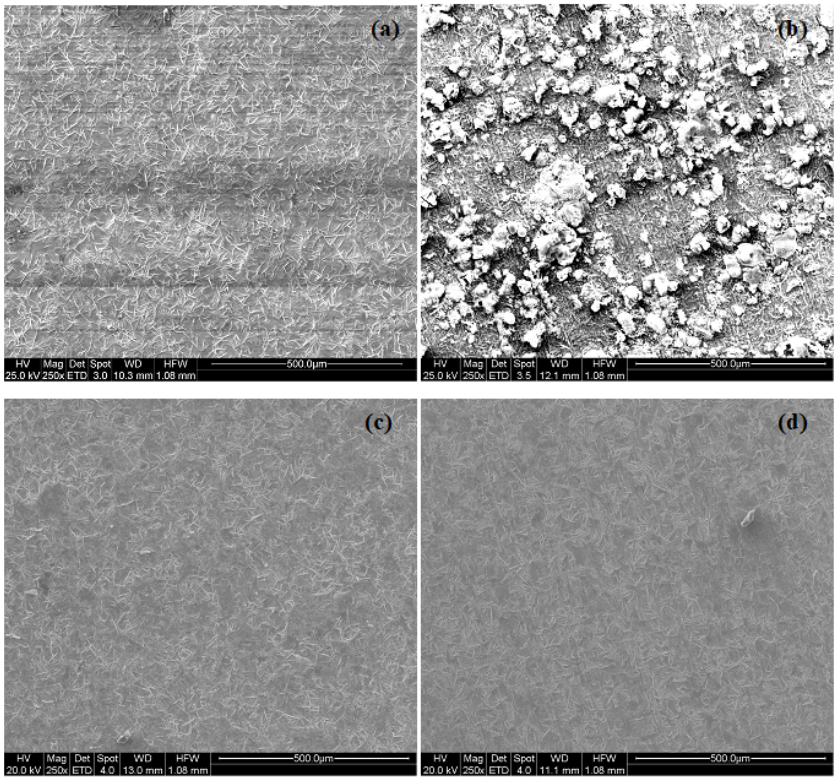

Figure 10

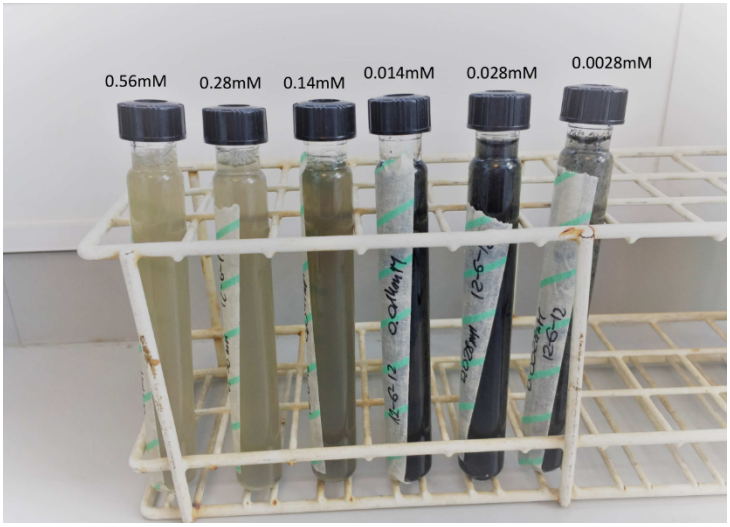

Figure 11

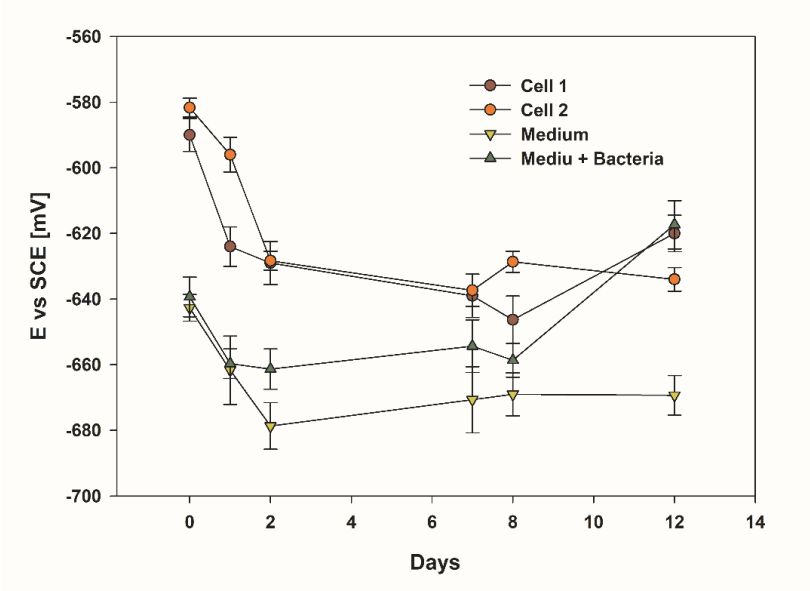

Figure 12

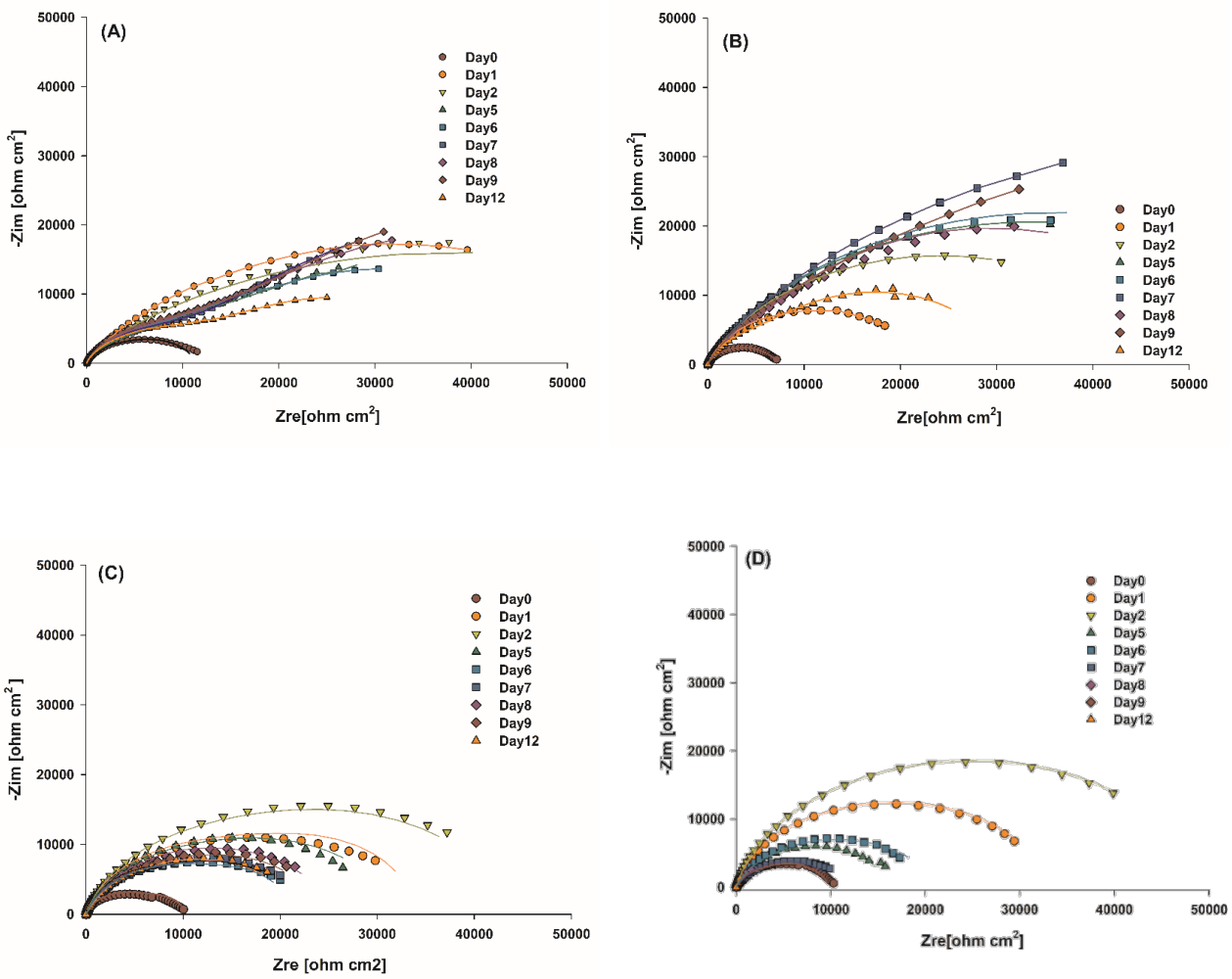
(A)
(B)
(C)
(D)
-Zim [ohm cm^2]
Zre[ohm cm^2]
Zre [ohm cm2]
Day0
Day1
Day2
Day5
Day6
Day7
Day8
Day9
Day12
0
10000
20000
30000
40000
50000

Figure 13

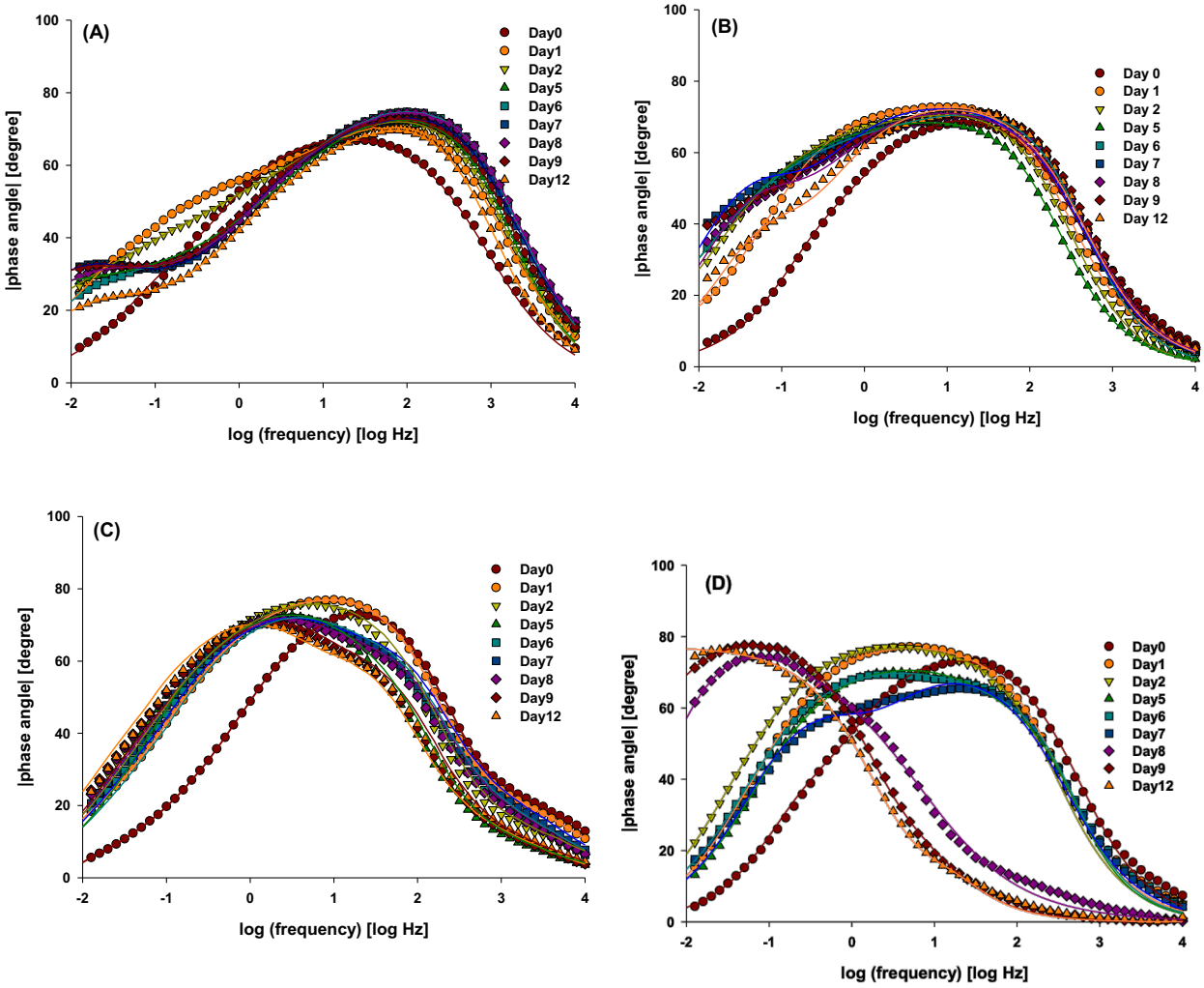
(A)
|phase angle| [degree]
log (frequency) [log Hz]
Day0
Day1
Day2
Day5
Day6
Day7
Day8
Day9
Day12
(B)
|phase angle| [degree]
log (frequency) [log Hz]
Day 0
Day 1
Day 2
Day 5
Day 6
Day 7
Day 8
Day 9
Day 12
(C)
|phase angle| [degree]
log (frequency) [log Hz]
Day0
Day1
Day2
Day5
Day6
Day7
Day8
Day9
Day12
(D)
|phase angle| [degree]
log (frequency) [log Hz]
Day0
Day1
Day2
Day5
Day6
Day7
Day8
Day9
Day12

Figure 14

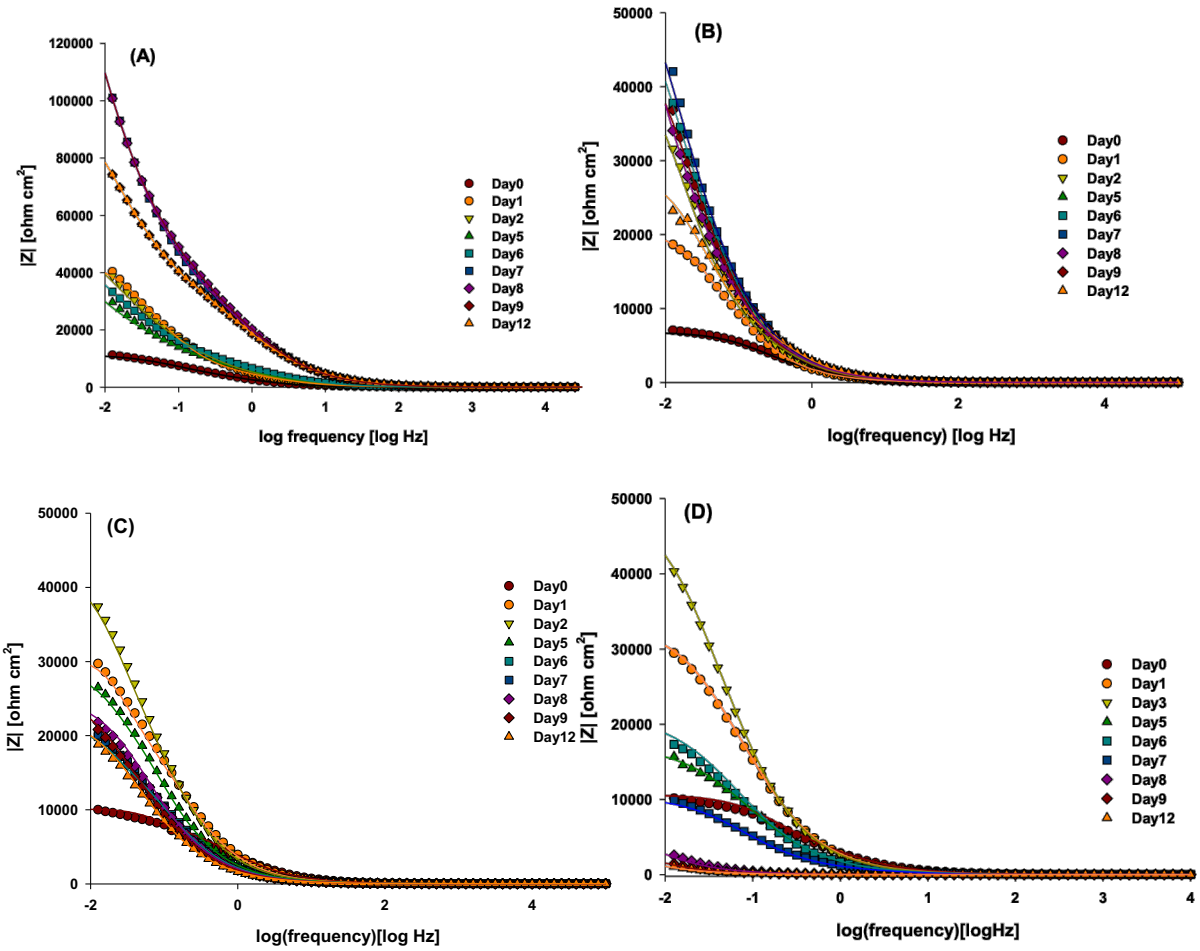
(A)
|Z| [ohm cm^2]
log frequency [log Hz]
Day0
Day1
Day2
Day5
Day6
Day7
Day8
Day9
Day12
(B)
|Z| [ohm cm^2]
log(frequency) [log Hz]
Day0
Day1
Day2
Day5
Day6
Day7
Day8
Day9
Day12
(C)
|Z| [ohm cm^2]
log(frequency)[log Hz]
Day0
Day1
Day2
Day5
Day6
Day7
Day8
Day9
Day12
(D)
|Z| [ohm cm^2]
log(frequency)[logHz]
Day0
Day1
Day3
Day5
Day6
Day7
Day8
Day9
Day12